Metal Chlorides in Ionic Liquid Solvents Convert Sugars to 5-Hydroxymethylfurfural

Haibo Zhao, *et al.*

Science **316**, 1597 (2007);
DOI: 10.1126/science.1141199

Science (print ISSN 0036-8075; online ISSN 1095-9203) is published weekly, except the last week in December, by the American Association for the Advancement of Science, 1200 New York Avenue NW, Washington, DC 20005.

8. M. M. Özer, Y. Jia, B. Wu, Z. Y. Zhang, H. H. Weitering, *Phys. Rev. B* **72**, 113409 (2005).
9. Y. Jia, B. Wu, H. H. Weitering, Z. Y. Zhang, *Phys. Rev. B* **74**, 035433 (2006).
10. L. Aballe, A. Barinov, A. Locatelli, S. Heun, M. Kiskinova, *Phys. Rev. Lett.* **93**, 196103 (2004).
11. A. G. Danese, F. G. Curti, R. A. Bartynski, *Phys. Rev. B* **70**, 165420 (2004).
12. Y. Guo *et al.*, *Science* **306**, 1915 (2004).
13. D. Eom, S. Qin, M. Y. Chou, C. K. Shih, *Phys. Rev. Lett.* **96**, 027005 (2006).
14. M. M. Özer, J. R. Thompson, H. H. Weitering, *Nat. Phys* **2**, 173 (2006).
15. M. M. Özer, J. R. Thompson, H. H. Weitering, *Phys. Rev. B* **74**, 235427 (2006).
16. N. Trivedi, N. W. Ashcroft, *Phys. Rev. B* **38**, 12298 (1988).
17. R. Hultgren, P. D. Desai, D. T. Hawkins, M. Gleiser, K. K. Kelley, *Selected Values of the Thermodynamic Properties of Binary Alloys* (American Society for Metals, Metals Park, OH, 1973).
18. G. Kresse, J. Hafner, *Phys. Rev. B* **47**, 558 (1993).
19. G. Kresse, J. Furthmuller, *Comput. Mater. Sci*. **6**, 15 (1996); and references therein.
20. J. P. Perdew, Y. Wang, *Phys. Rev. B* **45**, 13244 (1992).
21. Z. G. Suo, Z. Y. Zhang, *Phys. Rev. B* **45**, 13244 (1998).
22. J. Simonin, *Phys. Rev. B* **33**, 7830 (1986).
23. R. C. Dynes, J. M. Rowell, *Phys. Rev. B* **11**, 1884 (1975).
24. G. J. Dolan, J. Silcox, *Phys. Rev. Lett.* **30**, 603 (1973).
25. M. Tinkham, *Introduction to Superconductivity* (Dover, Mineola, NY, 1996).
26. Klaus Schröder, *CRC Handbook of Electrical Resistivities of Binary Metallic Alloys*, (CRC, Boca Raton FL, 1983). The room temperature resistivity ρ of $Pb_{1-x}Bi_x$ alloys increases linearly, 1.0 microhm cm/atomic % Bi for $x < \sim 0.2$. Assuming the phonon contribution does not change, the resistivity due to impurity scattering is 11 microhm cm for the 11% alloy, etc.
27. The only data points falling significantly below the straight line are for the 5-ML films, for which $H_{c2}(T)$ increases faster than linearly below T_c*.
28. V. M. Gvozdikov, *Low Temp. Phys.* **25**, 936 (1999).

29. This work was funded by NSF under contracts DMR-0244570 (M.M.O. and H.H.W.) and DMR-0606485 (Z.Z.); by the Division of Materials Sciences and Engineering (H.H.W., J.R.T., and Z.Z.), Office of Basic Energy Sciences, U.S. Department of Energy under contract DE-AC05-00OR22725 with Oak Ridge National Laboratory, managed by UT-Battelle, Limited Liability Corporation; and by National Science Foundation of China (Y.J.; grant no. 10574113).

6 March 2007; accepted 3 May 2007
10.1126/science.1142159

Metal Chlorides in Ionic Liquid Solvents Convert Sugars to 5-Hydroxymethylfurfural

Haibo Zhao, Johnathan E. Holladay, Heather Brown, Z. Conrad Zhang*

Replacing petroleum feedstocks by biomass requires efficient methods to convert carbohydrates to a variety of chemical compounds. We report the catalytic conversion of sugars giving high yield to 5-hydroxymethylfurfural (HMF), a versatile intermediate. Metal halides in 1-alkyl-3-methylimidazolium chloride are catalysts, among which chromium (II) chloride is found to be uniquely effective, leading to the conversion of glucose to HMF with a yield near 70%. A wide range of metal halides is found to catalyze the conversion of fructose to HMF. Only a negligible amount of levulinic acid is formed in these reactions.

A sustainable future for the chemical industry requires feedstocks based on renewable rather than steadily depleting sources. Inability to effectively transform five- and six-carbon carbohydrate building blocks derived from nature is a major barrier toward this challenging goal. Glucose and fructose, two abundant six-carbon sugar molecules, are potential feedstocks for this purpose, and recent efforts have focused on converting them to 5-hydroxymethylfurfural (HMF) (*1*), a versatile intermediate between biomass-based carbohydrate chemistry and petroleum-based industrial organic chemistry (*2*). HMF and its derivatives could potentially replace voluminously consumed petroleum-based building blocks (*3*), which are currently used to make plastics and fine chemicals. Recently, Dumesic and co-workers introduced the idea of using HMF as a key intermediate to produce liquid alkanes from renewable biomass resources (*4*). High production cost currently limits the availability and use of HMF industrially.

Institute for Interfacial Catalysis, Pacific Northwest National Laboratory, Post Office Box 999, Richland, WA 99352, USA.

*To whom correspondence should be addressed. E-mail: conrad.zhang@pnl.gov

A process to produce pure HMF from abundant renewable carbohydrates in high yield at low energy cost must be developed before a biorefinery platform can be built on the basis of this substrate. Current processes to produce HMF involve the use of acid catalysts and are mainly limited to fructose as feed (*5*–*7*). A drawback with acid catalysts is that they cause various side reactions, significantly increasing the cost of product purification. For example, in water under acidic conditions, HMF decomposes to levulinic acid and formic acid. Levulinic acid is particularly difficult to separate from HMF. Substituting glucose as a feed substantially reduces HMF yields and produces additional by-products (*8*, *9*).

A study by Antal and co-workers suggested that HMF is formed from dehydration of fructose in its furanose form (*10*) and occurs through a series of cyclic furan intermediates (*11*). Others have suggested HMF is formed through an acyclic mechanism proceeding through an enediol pathway (*11*–*14*). The enediol is proposed as an intermediate in the isomerization of glucose to fructose. Glucose has competing reaction pathways that lead to formation of by-products. In one pathway, dehydration forms nonfuran cyclic ethers; in another, C-C bond scission occurs through reverse aldol condensation (*14*). To obtain high HMF yields from glucose thus requires effective methods for selective in situ isomerization to fructose.

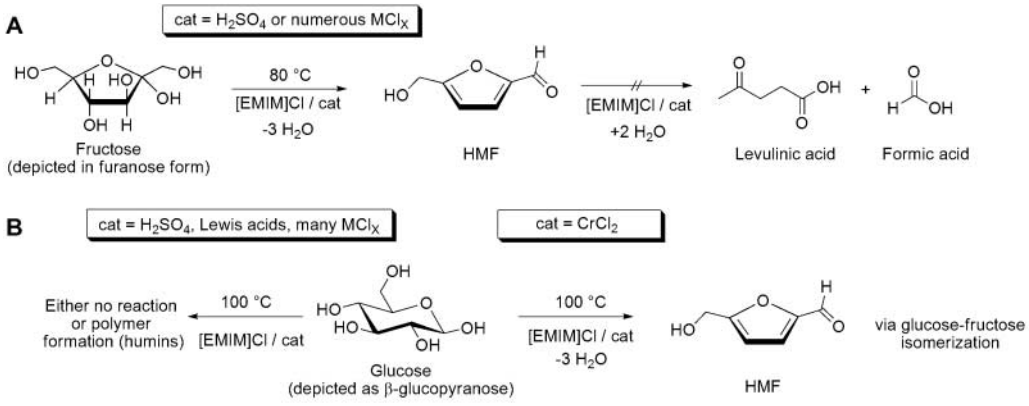

Fig. 1. (**A**) Fructose conversion to HMF at 80°C for 3 hours. Catalytic amounts of H_2SO_4 or various metal halides promote the chemistry. Very little levulinic acid is formed. (**B**) Glucose conversion to HMF at 100°C for 3 hours. $CrCl_2$ resulted in a 70% yield of HMF, whereas other catalysts such as H_2SO_4, Lewis acids, or other metal halides gave yields less than 10%.

HMF yield has been shown to increase significantly in systems that partition HMF from H_2O. Dumesic and co-workers, building on the work of several earlier researchers, demonstrated high yields from fructose by using strong polar organic solvents, such as dimethylsulfoxide (DMSO), in aqueous-organic reaction media (*7*). Other solvent systems have also shown promising results. HMF can be formed in high yields from fructose in 1-H-3-methylimidazolium chloride solvent, which also acts as an acidic catalyst (*15*, *16*). In sugar-solubilizing 1-alkyl-3-methylimidazolium chloride solvents, water is not needed as part of the solvent system, and the actual amount of H_2O present is reduced to the water formed during dehydration. By minimizing HMF exposure to acidic aqueous solutions at elevated temperatures, HMF yield loss to levulinic acid is kept very low.

In our own work, we have built upon this concept by using sugar-solubilizing high-purity 1-alkyl-3-methylimidazolium chloride, [AMIM]Cl, as a solvent class. Our method is distinguished from previous reports in that we observe high yields of HMF from fructose without added acid. Even more importantly, one of these solvent-catalyst systems is able to produce HMF in high yields from glucose, the first step in our ultimate goal of developing a system to generate HMF from complex biomass such as cellulose.

We tested the reactivity of fructose in three [AMIM]Cl solvents, where A represents octyl, butyl, or ethyl (*17*). Because [EMIM]Cl (E is ethyl) was equivalent or better than the other two solvents, we report results in this system (Fig. 1). Figure 2 shows the results of simply heating fructose and glucose in high-purity (99.5%) [EMIM]Cl (*18*). At sufficiently high-temperatures, fructose was converted to HMF, but the yield dropped substantially between 120° and 80°C. In contrast, glucose did not produce any substantial amount of HMF even at 180°C. When water was added to the solvent ([EMIM]Cl:H_2O = 5:1), glucose was effectively inert.

We were able to catalyze the dehydration of fructose at 80°C by addition of a catalytic amount of a number of metal halides (Fig. 1A). For example, HMF yields ranging from 63 to 83% were achieved in 3 hours when using 6 mole percent (mol %) loading (based on sugar) of $CrCl_2$, $CrCl_3$, $FeCl_2$, $FeCl_3$, CuCl, $CuCl_2$, VCl_3, $MoCl_3$, $PdCl_2$, $PtCl_2$, $PtCl_4$, $RuCl_3$, or $RhCl_3$ (fig. S1). The product mixtures were very clean: Yields of levulinic acid and α-angelicalactone were less than 0.08%. Not all metal halides were effective; for example, the alkali chlorides, $LaCl_3$ and $MnCl_2$, did not work.

We also looked at mineral and Lewis acid catalysts. Mineral acids were effective as expected. An 80% HMF yield was achieved when 18 mol % H_2SO_4 (relative to fructose) was used. A lower acid loading (1.8 mol %) gave 75% yield. In contrast, the widely studied $AlCl_3$–Lewis acid was not effective at molar ratios between 0.5 and 2 (*19*).

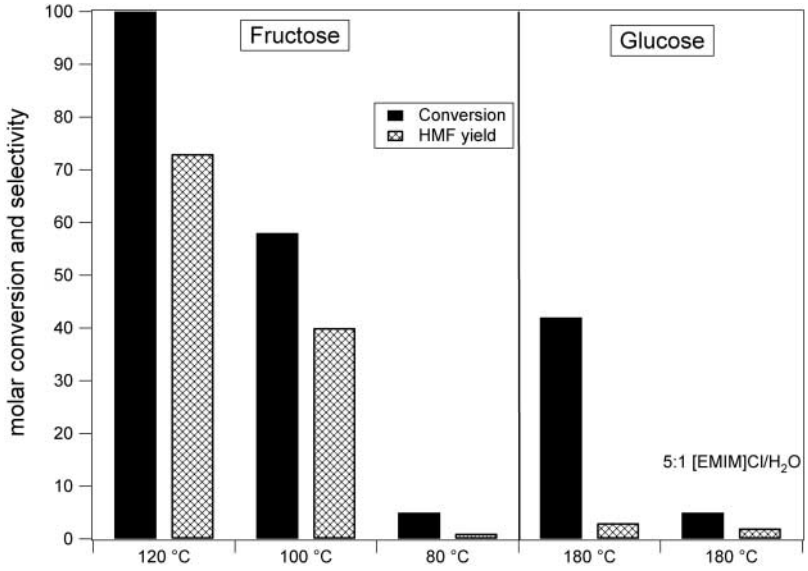

Fig. 2. Fructose and glucose conversion in [EMIM]Cl. Fifty mg of sugar was added to 500 mg of [EMIM]Cl and heated for 3 hours at the temperature indicated (no catalyst was added).

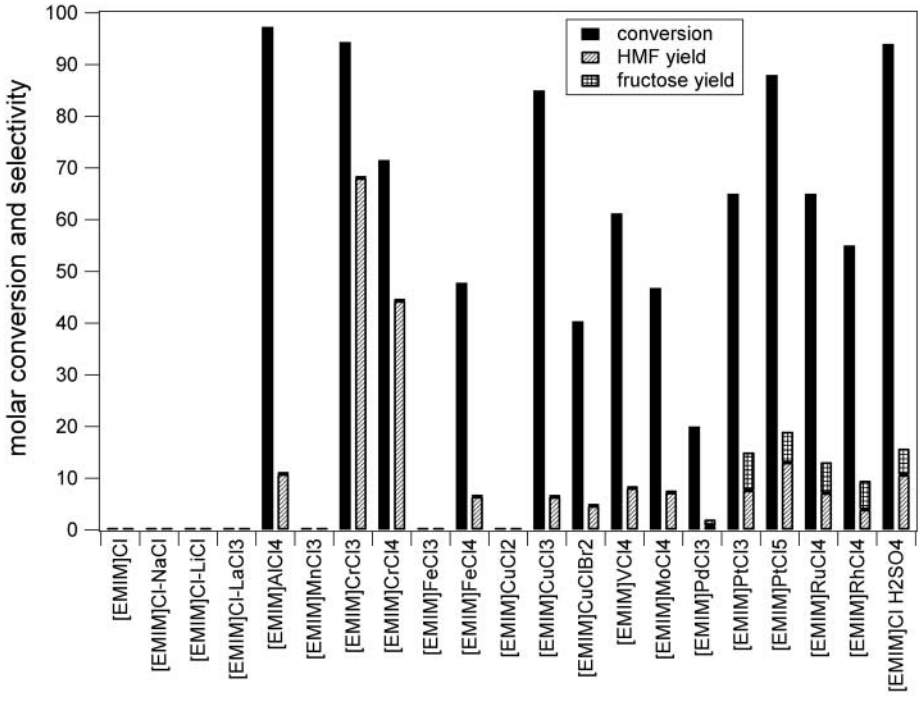

Fig. 3. Glucose conversion in [EMIM]Cl treated with numerous catalysts, most of which are effective for fructose dehydration. Only $CrCl_2$ leads to high HMF yield from glucose.

We repeated these studies with use of glucose as feed but raised the temperature to 100°C because of its lower reactivity (Fig. 1B). Twelve of the metal halides tested showed 40% conversion of glucose, but only one catalyst, $CrCl_2$, gave HMF in high yield (Fig. 3). HMF yield in [EMIM]Cl containing sulfuric acid or $AlCl_3$ was only 10%. The results were reproduced at least 20 times, and HMF yields for systems that did not contain $CrCl_x$ were consistently 10% or less, whereas $CrCl_2$ afforded HMF yields of 68 to 70%, a previously elusive efficiency from glucose. The products from the other catalysts included sugars such as mannose, dehydration products such as 1,6-anhydroglucose, and poorly characterized polymeric products [determined by ^{13}C nuclear magnetic resonance (NMR) spectroscopy].

For many of the catalysts, glucose conversion was high even though HMF yields were low (Fig. 2). We did a number of control experiments to demonstrate that the low HMF yield in these instances was not the result of HMF instability under the reaction conditions. After heating pure HMF at 100°C for 3 hours in the presence of

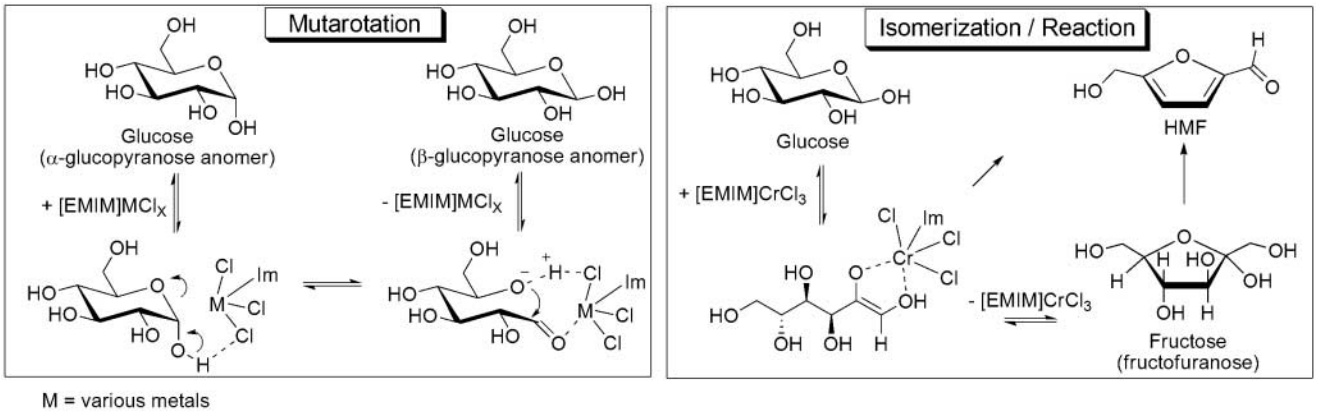

Fig. 4. Proposed metal halide interaction with glucose in [EMIM]Cl. $CuCl_2$ and $CrCl_2$ catalyze the mutarotation leading to interconversion of α- and β-glucopyranose anomers. $CrCl_2$ leads to the isomerization of glucopyranose to fructofuranose, followed by dehydration to HMF.

$CrCl_2$, 98% was recovered. When $CrCl_2$ was not added to [EMIM]Cl, HMF recovery was only 28%. Similar studies were done with other metal halides (HMF recoveries noted in parentheses): $CuCl_2$ (85%), VCl_4 (86%), and H_2SO_4 (98%). Interestingly, catalytic amounts of certain metal chlorides appear to play a role in stabilizing HMF. Catalysts usually enhance reactions; the concept of a catalytic amount of a substance, in less than stoichiometric quantities, blocking or quenching a reaction is most unusual.

In a second study, we examined HMF stability in the presence of sugar and catalyst. In these tests, xylose, a five-carbon sugar that cannot form HMF, was used. Fifty mg of a 1:1 mixture of HMF and xylose were added to 500 mg of the appropriate [EMIM]Cl-catalyst system and heated to 100°C for 3 hours. HMF recovery was high (recoveries given in parentheses): $CrCl_2$ (83%), $CuCl_2$ (90%), and VCl_4 (83%). HMF once again was more stable in the presence of metal halide; HMF recovery in [EMIM]Cl-xylose without catalyst was 66%. The data show that the low HMF yield cannot be accounted for by product instability under reaction conditions. Instead metal halides, such as $CuCl_2$ and VCl_4, catalyze undesired reaction pathways.

The singular effectiveness of catalytic amounts of $CrCl_2$ in [EMIM]Cl for the conversion of glucose to HMF was unanticipated. In an effort to understand the results, we turned to spectroscopy. Our NMR study showed that the glucose starting material, when dissolved in the [EMIM]Cl solvent, is predominantly an α-anomer. Solvation of sugars occurs through hydrogen bonding of chloride ions of the solvent with the carbohydrate hydroxy groups (*20*). However, this interaction is insufficient to cause mutarotation (that is, α- to β-anomer conversion; Fig. 4). Little interconversion of the α- and β-anomers occurred in [EMIM]Cl, even after several hours at 80°C. However, in the presence of a catalytic amount of $CuCl_2$ or $CrCl_2$, mutarotation leading to an equilibrium mixture of anomers was rapid (figs. S2 and S3). In the ^{1}H NMR spectrum, the six –OH resonances were sharp. In the presence of catalytic amounts of $CuCl_2$ the –OH resonances shifted upfield and were very broad, indicating exchange through interactions with the metal (*21*).

[AMIM]Cl structures are known to be weakly coordinating (*22*) and do not compete with sugar for the binding of the metal chlorides. Our hypothesis is that sugar-metal coordination is responsible for the catalysis. To characterize the prevailing coordination bonding motif, we examined the effect of adding stoichiometric glycerol or glyceraldehyde to glucose solutions. Glucose can be thought of as a glycerol molecule attached to a glyceraldehyde molecule. By using NMR spectroscopy, we confirmed that glyceraldehyde exists as a hemiacetal dimer in [EMIM]Cl, which makes it a very good mimic for glucopyranose. In the competition reactions, glycerol had no impact on the catalysis, and 70% yield of HMF was achieved from glucose. Glyceraldehyde, however, did affect the chemistry: Reaction inhibition was observed. HMF yield was reduced to less than 20%, and glucose conversion was reduced to ~60%. In addition, we evaluated 2,2′-bipyridine as a strongly coordinating ligand (5:1 molar ratio to Cr). In the presence of the strongly coordinating ligand, the reaction essentially shut down: HMF yield was less than 2%, and glucose recovery was 90%. The results of the glycerol and glyceraldehyde competition studies show that the metal interacts with the hemiacetal portion of glucopyranose but that there is little interaction with the polyalcohol portion of the sugar.

Although we lack a clear picture of why $CrCl_2$ is a singularly effective catalyst in [EMIM]Cl solvent, we are able to offer some insights into the mechanism. We studied the kinetic behavior of $CrCl_2$, $CuCl_2$, and $FeCl_2$, which show dramatic differences in their reaction pathways (fig. S4). The rate of glucose conversion was highest with $CrCl_2$; $CuCl_2$ was reactive, but mainly gave condensation products; and $FeCl_2$ showed no reaction. With $CuCl_2$, multiple products were formed, including mannose, HMF, and 1,6-anhydroglucose. This diverse product mix suggests that $CuCl_2$ coordination with the sugar is different from that of $CrCl_2$.

To explain the results with $CrCl_2$, we show a mechanism consistent with the data (Fig. 4). Because only 0.5% by weight of $CrCl_2$ was added to the solvents, the plausible formation of $[EMIM]^+CrCl_3^-$ would consume only an equimolar amount of [EMIM]Cl with respect to $CrCl_2$, according to Eq. 1:

$$[EMIM]Cl + CrCl_2 \rightarrow [EMIM]CrCl_3 \quad (1)$$

We propose that the $CrCl_3^-$ anion plays a role in proton transfer, facilitating mutarotation of glucose in [EMIM]. A critical role of $CrCl_3^-$ is to effect a formal hydride transfer, leading to isomerization of glucose to fructose. As discussed above, all other tested metal chlorides failed to convert glucose to fructose in the [EMIM]Cl solvent. A chromium enolate may be the key intermediate (*23*). Once fructose is formed, dehydration of fructofuranose is rapid in the presence of the catalyst in the solvent. Lowering the dielectric constant of the media by addition of organic solvents (10:1 glycerol to [EMIM]Cl) results in loss of catalytic activity. Other metal halides also bind to glucose. However, they promote alternative reaction paths that do not lead to the desired products.

References and Notes

1. T. A. Werpy *et al.*, "Top value added chemicals from biomass" [U.S. Department of Energy (DOE) report number DOE/GO-102004-1992, Golden, CO, 2004; www.nrel.gov/docs/fy04osti/35523.pdf.
2. B. Kamm, M. Kamm, M. Schmidt, T. Hirth, M. Schulze, in *Biorefineries: Industrial Processes and Products*, B. Kamm, P. R. Gruber, M. Kamm, Eds. (Wiley, Weinheim, Germany, 2006), vol. 2, pp. 97–149.
3. M. Bicker, J. Hirth, H. Vogel, *Green Chem.* **5**, 280 (2003).
4. G. W. Huber, J. N. Chheda, C. J. Barrett, J. A. Dumesic, *Science* **308**, 1446 (2005).
5. F. S. Asghari, H. Yoshida, *Ind. Eng. Chem. Res.* **45**, 2163 (2006).
6. B. F. M. Kuster, *Starch Starke* **42**, 314 (1990).
7. Y. Róman-Leshkov, J. N. Chheda, J. A. Dumesic, *Science* **312**, 1933 (2006).
8. S. K. Tyrlik, D. Szerszen, M. Olejnik, W. Danikiewicz, *Carbohydr. Res.* **315**, 268 (1999).
9. M. Watanabe *et al.*, *Carbohydr. Res.* **340**, 1925 (2005).

10. Sugars exist as cyclic structures in solution. In H_2O, fructose is about 68% fructopyranose and 32% fructofuranose, and glucose is about 99% glucopyranose and 1% glucofuranose (*24*). In this paper, we use the terms fructose and glucose in reference to the sugars in any of their conformers.
11. M. J. Antal, W. S. L. Mok, G. N. Richards, *Carbohydr. Res.* **199**, 91 (1990).
12. Z. Srokol *et al.*, *Carbohydr. Res.* **339**, 1717 (2004).
13. B. M. Kabyemela, T. Adschiri, R. M. Malaluan, K. Arai, *Ind. Eng. Chem. Res.* **38**, 2888 (1999).
14. B. M. Kabyemela, T. Adschiri, R. M. Malaluan, K. Arai, *Ind. Eng. Chem. Res.* **36**, 1552 (1997).
15. C. Lansalot-Matras, C. Moreau, *Catal. Commun.* **4**, 517 (2003).
16. C. Moreau, A. Finiels, L. Vanoye, *J. Mol. Catal. Chem.* **253**, 165 (2006).
17. Materials and methods can be found on *Science* Online.
18. The [EMIM]Cl in this study gave a pH of 7 when mixed with H_2O in a 1:1 ratio. The pH of less-pure ionic liquids ranged from neutral to acidic.
19. At a mole ratio of 2, the melt is a Lewis acid (*25*).
20. R. C. Remsing, R. P. Swatloski, R. D. Rogers, G. Moyna, *Chem. Commun.* 1271 (2006).
21. $CuCl_2$ was used to study sugar-metal interactions, because chromium is strongly paramagnetic and the line-broadened spectrum was uninformative.
22. Z. C. Zhang, *Adv. Catal.* **49**, 153 (2006).
23. L. Mønsted, O. Mønsted, *Inorg. Chem.* **44**, 1950 (2005).
24. S. J. Angyal, *Adv. Carbohydr. Chem. Biochem.* **42**, 63 (1984).
25. K. M. Dieter, C. J. Dymek Jr., N. E. Heimer, J. W. Rovang, J. S. Wilkes, *J. Am. Chem. Soc.* **110**, 2722 (1988).

26. This work was supported by the Laboratory Directed Research and Development Program at the Pacific Northwest National Laboratory (PNNL), a multiprogram national laboratory operated by Battelle for the U.S. DOE under contract no. DE-AC06-76RL01830. Part of the research described in this paper was performed at the Environmental Molecular Science Laboratory, a national scientific user facility located at PNNL. We thank A. Appel for running the NMR experiments.

Supporting Online Material

www.sciencemag.org/cgi/content/full/316/5831/1597/DC1
Materials and Methods
Figs. S1 to S4

12 February 2007; accepted 18 April 2007
10.1126/science.1141199

Extracellular Proteins Limit the Dispersal of Biogenic Nanoparticles

John W. Moreau,[1]*† Peter K. Weber,[2] Michael C. Martin,[3] Benjamin Gilbert,[4] Ian D. Hutcheon,[2] Jillian F. Banfield[1,4,5]

High–spatial-resolution secondary ion microprobe spectrometry, synchrotron radiation–based Fourier-transform infrared spectroscopy, and polyacrylamide gel analysis demonstrated the intimate association of proteins with spheroidal aggregates of biogenic zinc sulfide nanocrystals, an example of extracellular biomineralization. Experiments involving synthetic zinc sulfide nanoparticles and representative amino acids indicated a driving role for cysteine in rapid nanoparticle aggregation. These findings suggest that microbially derived extracellular proteins can limit the dispersal of nanoparticulate metal-bearing phases, such as the mineral products of bioremediation, that may otherwise be transported away from their source by subsurface fluid flow.

Sulfate-reducing bacteria can lower the concentrations of metals in anoxic waters by sequestering metals into nanoparticles (*1*–*3*). However, these particles are potentially highly mobile because of their small size (*4*) and can redissolve quickly if conditions change (*5*). Sulfide nanoparticles may be <2 nm in diameter [comparable in size to aqueous molecular clusters (*6*)]; most have a diameter of 2 to 6 nm (*2*, *7*). Aggregation can restrict nanoparticle transport by inducing settling (*8*, *9*), and it can drive crystal growth, leading to decreased solubility (*10, 11*). Some organics can promote aggregation. Amine-bearing molecules, for example, have been shown to organize sulfide nanoparticles into semiconductor nanowires (*12*).We investigated the hypothesis that natural organic matter contributes to the formation of densely aggregated nanoparticulate ZnS spheroids and is preserved in nanometer-scale pores (*7*). We used micro-analytical and direct isolation approaches to analyze nanoparticle aggregates formed in natural sulfate-reducing bacterial biofilms (*7*, *13*). We also experimentally evaluated the potential for various amino acids to induce rapid aggregation of metal-sulfide nanoparticles.

We examined sulfate-reducing bacteria–dominated biofilms collected from the Piquette Pb and Zn Mine, a flooded system (pH ~7, ~8°C) in southwestern Wisconsin (*13*). Ultramicrotomed biofilm sections that contained spheroidal aggregates of biogenic ZnS nanoparticles (figs. S1 to S4) were imaged with transmission electron microscopy (TEM) before in situ elemental microanalysis with secondary ion mass spectrometry at a spatial resolution of ~50 nm (NanoSIMS) (*14*). N in the samples was detected by NanoSIMS as CN^-, NO^-, and NS^- secondary ions and was quantified by comparison to reference samples (*14*, *15*).

A comparison of TEM images with NanoSIMS S distribution maps demonstrates that ZnS spheroids are the only structures within the biofilm that contain significant S concentrations (Fig. 1, A to C). The composite NanoSIMS data show the intimate association of N with biofilm ZnS (Fig. 1, A to C); N is present throughout these aggregates at significantly higher levels than in abiotic ZnS reference materials (Fig. 1, D and E). Pores in the ZnS spheroids appear as low–diffraction-contrast features in TEM images because of a lower concentration of sphalerite nanoparticles (fig. S2). Porous regions are associated with the highest N concentrations (Fig. 1, B and C). N concentration measurements for individual spheroids varied by 14% (relative SD, $n = 134$ spheroids), as compared with an average measurement precision of 4%, for individual ZnS aggregates with an average diameter of 700 nm. We estimated an average N concentration for all analyzed biofilm ZnS spheroids of 1.6 weight % (wt %), with a 95% confidence interval of 0.8 to 3 wt % (*14*). By comparison, the average N concentration of synthetic ZnS aggregates was ~100 times lower than it was for biofilm ZnS spheroids.

The small nitrate concentration of mine water (~3 μg/g) was removed from the biofilm during sample processing and was therefore not expected to be the source of N in ZnS. To test this prediction, we analyzed the spheroids for NO^-, relative to CN^- (*14*). The CN^-/NO^- ratio for a reference sample of KNO_3 dissolved in graphite (*14*) ranged from <1 to 200, with a median ratio of ~6. The average CN^-/NO^- ratio of bacterial spores, an organic N reference, was 2950 ± 520 (SD). The average CN^-/NO^- ratio of the biofilm ZnS was 3300 ± 870 (SD). Measurement precision for CN^-/NO^- in the biofilm ZnS was similar to sample variability because of low NO^- secondary-ion intensities. Based on these analyses, we concluded that N in the biofilm ZnS was present neither as nitrate nor nitrite and was therefore organic in nature (*14*). This conclusion was further supported by the presence of amide absorption features in the infrared spectra discussed below. From the average N content of ZnS estimated above and an average amino acid N concentration of ~11 wt %, the ZnS spheroids contained ~14 wt % amino acids.

Areas with cell-like morphologies enriched in N (Fig. 1) and P (fig. S8) are interpreted as being either whole or degraded microbial cells. These features are morphologically distinct from ZnS spheroids, arguing against spheroid formation by nanoparticle encrustation and infilling of cells. We inferred that the spheroids formed by the aggregation of biogenic ZnS nanoparticles (*13*) with extracellular polypeptides or proteins. This process may have involved the adsorption of amino acids or peptides onto nanoparticle surfaces (*16*) or the

[1]Department of Earth and Planetary Science, University of California Berkeley, Berkeley, CA 94720, USA. [2]Glenn T. Seaborg Institute, Lawrence Livermore National Laboratory (LLNL), Livermore, CA 94551, USA. [3]Advanced Light Source, Lawrence Berkeley National Laboratory, Berkeley, CA 94720, USA. [4]Earth Science Division, Lawrence Berkeley National Laboratory, Berkeley, CA 94720, USA. [5]Department of Environmental Science, Policy, and Management, University of California Berkeley, Berkeley, CA 94720, USA.

*Present address: U. S. Geological Survey, Water Resources Division, 8505 Research Way, Middleton, WI 53562, USA. †To whom correspondence should be addressed. E-mail: jwmoreau@usgs.gov